Available online at www.sciencedirect.com
SCIENCE DIRECT®
Biochemical and Biophysical Research Communications 330 (2005) 39–45
BBRC
www.elsevier.com/locate/ybbrc

Design of recombinant protein-based SARS-CoV entry inhibitors targeting the heptad-repeat regions of the spike protein S2 domain

Ling Ni [a,b], Jieqing Zhu [a], Junjie Zhang [a], Meng Yan [a], George F. Gao [a,*], Po Tien [a,*]

[a] Department of Molecular Virology, Institute of Microbiology, Chinese Academy of Sciences, Beijing 100080, PR China
[b] Graduate School of the Chinese Academy of Sciences, PR China

Received 1 February 2005

Abstract

Entry of SARS-CoV into a target cell is initiated by binding of the S1 domain of spike protein to a receptor, followed by conformational changes of the spike protein S2 domain, resulting in the formation of a six-helix bundle by the heptad-repeat (HR1 and HR2) regions. Our previous studies have demonstrated that peptides derived from HR2 region could inhibit SARS-CoV entry. However, synthesis of these peptides is at high cost. In this study, we designed two recombinant proteins, one containing two HR1 and one HR2 peptides (denoted HR121), and the other consisting of two HR2 and one HR1 peptides (designated HR212). These two proteins could be easily purified with the low cost of production, exhibiting high stability and potent inhibitory activity on entry of the HIV/SARS pseudoviruses with IC_{50} values of 4.13 and 0.95 μM, respectively. These features suggest that HR121 and HR212 can serve as potent inhibitors of SARS-CoV entry.

Keywords: Design; SARS-CoV; Protein inhibitors; Heptad-repeat regions; Spike protein; Pseudotyped virus

Severe acute respiratory syndrome (SARS) is a life-threatening form of atypical pneumonia [1,2]. It has seriously threatened public health and socioeconomic stability. More than 8000 people were infected and 774 worldwide, mostly in Asia, were killed by the disease before it was brought under control in July between the winter and spring in 2002–2003 (WHO website: www.who.int). However, the current therapeutic agents for SARS-CoV infection are mainly hormone agents. Despite the success of these drugs in treating SARS, they also cause many sequelae, such as arthralgia [3]. Accordingly, new types of therapeutics are needed.

SARS is caused by a novel coronavirus, SARS-CoV [4–9]. Coronaviruses, belonging to coronaviridae family, are enveloped positive-strand RNA viruses. The enveloped glycoproteins of the enveloped viruses initiate entry of viruses into their host cells by binding to cell surface receptors followed by conformation changes leading to membrane fusion and delivery of the genome in the cytoplasm [10–14]. As for SARS-CoV, the fusion process is mediated by the spike protein on the surface of the virus [15]. The spike protein is a typical class I viral fusion protein just like the transmembrane glycoprotein of many other enveloped viruses [14,16]. It is composed of two subunits: S1, a surface subunit that binds to the host cell surface receptor; and S2, a transmembrane subunit that ultimately inserts into the host cell membrane and promotes the fusion events. The S2 domain of the spike protein contains two helical regions, one near the amino terminus (HR1) and the other near the carboxy terminus (HR2), both of which are well conserved. In the late stages of membrane fusion, these two

* Corresponding authors. Fax: +86 10 62622101.
E-mail addresses: ggao66@yahoo.com (G.F. Gao), tienpo@sun.im.ac.cn (P. Tien).

0006-291X/$ - see front matter © 2005 Elsevier Inc. All rights reserved.
doi:10.1016/j.bbrc.2005.02.117

regions interact with each other in an antiparallel manner to form a trimer-of-hairpins that shares significant similarity with the fusion core structure of MHV spike protein and other viral fusion proteins [17]. This facilitates the juxtaposition of the virus and cell membranes, leading to membrane fusion. Moreover, peptides derived from HR2 region of the spike protein have been found to have inhibitory activity just as those of retrovirus and paramyxovirus fusion protein [18–21]. HR2 peptides likely inhibit formation of the trimer-of-hairpins in a dominant-negative manner by binding to HR1 region just like T-20 (Fig. 1A). T-20 is the first inhibitor to be approved by the US Food and Drug Administration (FDA) and European Commission for the treatment of HIV infection in adults and children aged 6 years and older. However, one of the major limitations of T-20 is the difficulty of peptide synthesis, resulting in high cost of production and insufficiency of supplies [22]. Accordingly, it is necessary to find the analogs of these peptide inhibitors with the same fusion-inhibitory activity, but the production is at low cost.

Recombinant proteins that contain the HR1 and HR2 segments of HIV-1 gp41 separated by a short, hydrophilic, six-residue linker (HR1-HR2, 2-helix) have been produced and shown to fold into thermally stable six-helix bundles [23]. We have also previously shown that 2-helix proteins from a number of paramyxovirus F proteins, such as NDV [24], Mumps virus [25], Measles virus [26], and Menangle virus [27], could also form typical six-helix bundles and be used successfully for crystallization. Based on our previous constructs, we designed two proteins, HR121 (HR1-HR2-HR1) and HR212 (HR2-HR1-HR2), analogous to HR1 and HR2, respectively. One more HR sequence was linked with 2-helix, which led to the formation of HR121 and HR212. In this study, we used a GST-fusion system to express HR121 and HR212 separately in an *Escherichia coli* (*E. coli*). HR121 and HR212 could be easily expressed and purified, exhibiting stable α-helical structure in solution and potent inhibitory activity on entry of the HIV/SARS pseudotyped virus.

Materials and methods

Plasmids and cell lines. pNL43LucE$^-$R$^-$ (HIV-luc) and the codon optimized SARS-CoV S protein expression plasmid pcTSh (strain BJ01, GenBank Accession No. AY278488, a gift from Dr. Hongkui Deng) were utilized in the production of HIV/SARS pseudoviruses. 293T cells used in pseudotyped virus generation and Huh 7 cells used

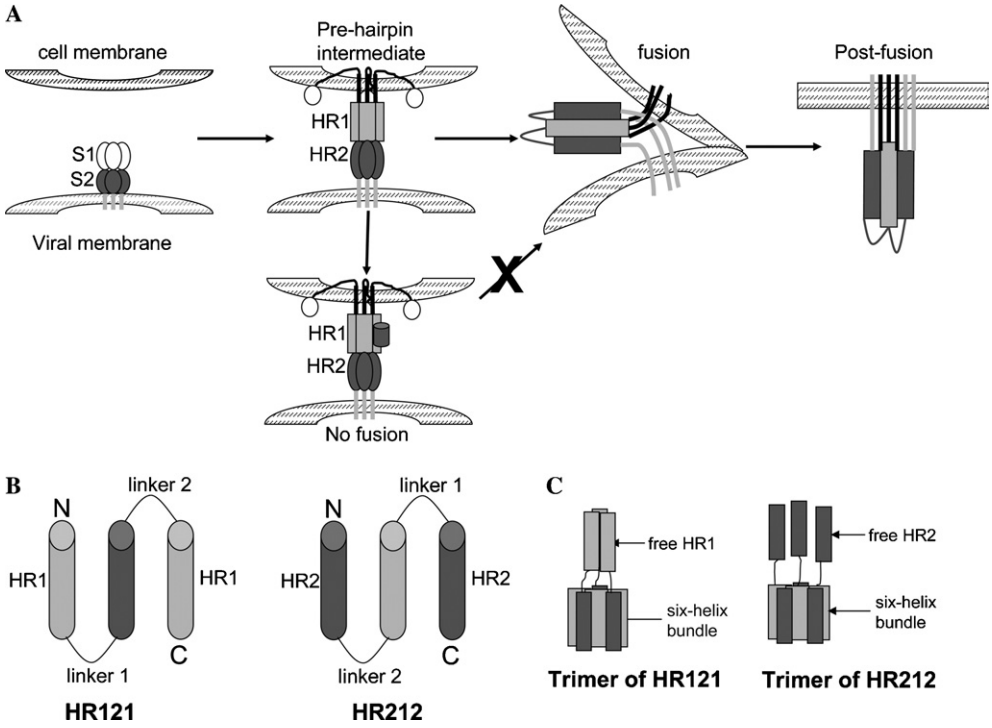

Fig. 1. Target SARS-CoV membrane fusion. (A) A schematic model of SARS-CoV membrane fusion [21]. In the prehairpin intermediate, the central coiled-coil formed by three HR1s and three HR2s was exposed and could be targeted by exogenous HRs. In the absence of inhibitors, this transient state ultimately collapsed into a six-helix bundle that brought the HR1 and HR2 regions into close proximity, promoting membrane fusion. The entry inhibitors (black cylinder) targeting HR1 regions prevented the formation of the six-helix bundle. (B) HR121 contained two HR1 segments and one HR2 segment alternatively linked with the short Gly/Ser peptide sequences, while HR212 consisted of two HR2 segments and one HR1 segment. The sequences of HR1 and HR2 for constructing HR121 and HR212 were peptides N35 and C35, respectively; linker 1, GGSGG; and linker 2, SGGRGG. (C) Schematic models of the trimer of HR121 (left) and HR212 (right). Both HR121 and HR212 assembled into six-helix bundles with free HR1s or HR2s.

in cell–cell fusion assays were cultured in Dulbecco's modified Eagle's medium supplemented with 10% fetal bovine serum.

Gene construction. Learn Coil-VMF program [28] was used to predict the amino acid sequences of HR1 and HR2 regions. Genes encoding amino acids 898–1005 for HR1 (N108), 900–943 for HR1 (N44), 916–950 for HR1 (N35), 1149–1186 for HR2 (C38), and 1151–1185 for HR2 (C35) were amplified by PCR from pcTSh. Based on Tripet's finding [29], we selected N35 and C35 to construct HR121 (N35-C35-N35) and HR212 (C35-N35-C35). HR121 consisted of two N35 segments and one C35 segment alternatively linked with the short peptide sequences, while HR212 consisted of two C35 segments and one N35 segment (Fig. 1B). The genes encoding the two proteins were then subcloned into *E. coli* expression vector pGEX-6P-1 by two restriction enzyme sites of *Eco*RI and *Xho*I. A stop codon was introduced before the *Xho*I site. This cloning strategy yielded glutathione *S*-transferase (GST) fusion proteins and the fusion proteins were named after GST-HR121 and GST-HR212, respectively. N108, N44, and C38 were subcloned into the *Bam*HI/*Xho*I site of pET-30a and yielded the proteins with N-terminal 6× his-tag, thrombin, and enterokinase cleavage sites. The purified proteins were named after N108-30a, N44-30a, and C38-30a, respectively.

Protein expression and purification. The recombinant plasmids of pGEX-6p-1-HR121, pGEX-6p-1-HR212 and the plasmid pGEX-6p-1 itself were transformed into *E. coil* strain BL21 (DE3). Single colony from the respective transformation was grown at 37 °C in 2× YT to an optical density (OD) at 600 nm of 0.8–1.0 and then induced with 0.5 mM IPTG at 20 °C for 4 h. Bacterial cells were harvested and lysed by sonication in phosphate-buffered saline (PBS, 10 mM sodium phosphate, pH 7.3; 150 mM NaCl). Triton X-100 was then added to a final concentration of 1% and the lysate was incubated for 30 min on ice and subsequently clarified by centrifugation at 12,000*g* for 15 min at 4°C. The clarified supernatants were applied to Glutathione-Sepharose 4B affinity column (Pharmacia). The column was then washed with 10 bed volumes of PBS and eluted with reduced L-glutathione (15 mM). The HR121 and HR212 proteins were subsequently cleaved from the fusion proteins by GST-fusion rhino-virus 3C protease (GST-3C), kindly provided by Drs. K. Hudson and J. Heath, and were loaded on glutathione–Sepharose 4B affinity column again to remove GST and GST-3C. The samples were then purified by a Hiload Superdex G75 column (Pharmacia) running on Akta Explorer FPLC system (Amersham-Pharmacia). The fractions of the peak were collected and run on 12% SDS–PAGE. The peak molecular weight was estimated by comparison with the protein standards (Pharmacia) running on the same column. The clarified supernatants of N108, N44, and C38 were applied on Ni-chelated Sepharose affinity column (Pharmacia). The column was then washed by PBS over 10 column volumes and eluted with imidazole (500, 300, and 200 mM, respectively).

Chemical cross-linking. This was done according to the method described earlier [26]. Briefly, the gel-filtration purified HR121 and HR212 were dialyzed against cross-linking buffer (50 mM Hepes, pH 8.3; 100 mM NaCl) separately and concentrated to about 2 mg/ml by ultrafiltration (10 kDa cut-off). Proteins were cross-linked with ethylene glycol bis (succinimidyl succinate) (EGS, dissolved in DMSO) (Sigma). The reactions were incubated for 1 h on ice at concentrations of 0, 0.1, 0.2, 0.4, 0.8, and 1.2 mM EGS and stopped by 50 mM glycine. Cross-linked products were analyzed under reducing conditions on 12% SDS–PAGE.

CD spectroscopy. CD spectra were performed on a Jasco J-715 spectrophotometer with proteins in PBS. Wavelength spectra were recorded at 37 °C using a 0.1 cm path-length cuvette. The protein concentration used for this was 10 μg/ml.

GST pull-down assay. Excess N108-30a and C38-30a in classified bacterium supernatants were, respectively, mixed with GST-HR121 and GST-HR212. The mixtures were incubated for 1 h at room temperature before glutathione–Sepharose 4B affinity gel was added. The gel with the protein mixtures was then incubated with gentle agitation at room temperature for 30 min. The suspension was centrifuged at 500*g* for 5 min to sediment the gel with adsorbed fusion protein complexes. The column was then washed with 10 bed volumes of PBS and eluted with reduced L-glutathione. The eluted samples were analyzed by SDS–PAGE.

Inhibition of HIV/SARS pseudovirus entry by HR121 and HR212. HIV/SARS pseudovirus was produced as described by Deng [30]. pNL43LucE$^-$R$^-$ and pcTSh were co-transfected into 293T cells. Forty eight hours later, HIV/SARS pseudovirus-containing supernatant was mixed with serially diluted protein. The virus/protein mixture was then transferred to 24-well plates seeded with Huh 7 cells. Three hours later, the medium was replaced. Following 2 days incubation at 37 °C, the cells were harvested in lysis buffer, analyzed for luciferase activity by the addition of luciferase substrate, and measured for 10 s in a TD-20/10 luminometer. The IC_{50} values were calculated by fitting the HR121 and HR212 titration data Langmuir function {normalized luciferase activity $= 1/(1 + C/IC_{50})$}.

Results and discussion

Design of HR121 and HR212

The trimeric core of the ectodomain of SARS-CoV S2, 2-helix, which has been solved crystallographically [17], comprises residues 900–948 (HR1) and 1145–1184 (HR2) of SARS-CoV S2 covalently linked to a 22-residue linker. The structure forms a thermostable trimer of hairpins in which HR1 and HR2 are entirely helical and arranged in a six-helix bundle. We have made use of the 2-helix core as a scaffold to link another HR1 to its C terminus and another HR2 to its N terminus, respectively (Fig. 1C). The rational for this design is that three HR1s or HR2s will be stabilized as a consequence of it being covalently linked to the S2 ectodomain core by a flexible linker. Then the stability of the designed HR212 and HR121 will be improved.

Both HR121 and HR212 were expressed as soluble stable proteins

In this study, to produce HR121 and HR212, we used the recombinant *E. coli* expression system which was able to provide protein products in large quantities at low cost. The designed two proteins were expressed as GST fusion proteins in soluble form and it was easy to elute GST-HR121 and GST-HR212 from the glutathione–Sepharose column by the normal elution buffer (15 mM reduced glutathione, 50 mM Tris–HCl, pH 8.0). Moreover, the two GST fusion proteins could be easily cleaved by GST-3C protease (Fig. 2). Namely, the free HR121 and HR212 were easily expressed and purified in large quantities at low cost.

The purified HR121 and HR212 were then analyzed in gel filtration for estimation of the molecular weight and the assembly character. The elution peaks of both HR121 and HR212 proteins were just after the peak position corresponding to 52 kDa, while the calculated molecular weights of HR121 and HR212 were 12.4

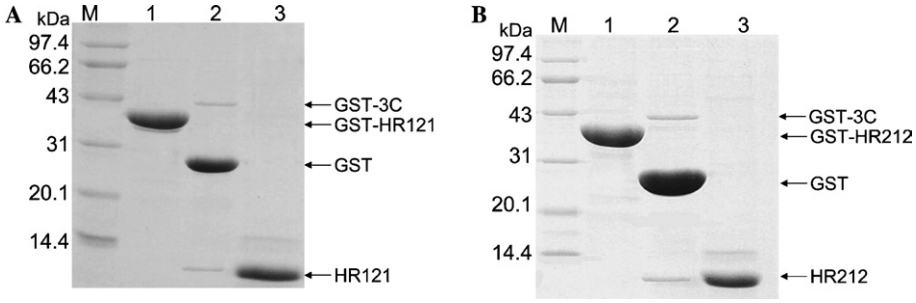

Fig. 2. SDS–PAGE analysis of the purified proteins. Both HR121 (A) and HR212 (B) were expressed as GST fusion proteins and cleaved by GST-3C. Lane M, protein markers (in kDa); lane 1, GST fusion protein with HR121 or HR212; lane 2, the GST fusion proteins digested after GST-3C; and lane 3, the free HR121 and HR212.

and 12.6 kDa, respectively, which indicates that both HR121 and HR212 could form oligomers, probably trimers (Figs. 3A and B). Subsequently, chemical cross-linking demonstrated that HR121 and HR212 could indeed form trimer (Figs. 3C and D), although the monomer/dimer bands did not completely disappear even in high concentrations of the cross-linker. However, the density of the trimer band tended to get thicker with the gradual increase of the cross-linker concentrations. The molecular weight of the cross-linked trimer was around 38 kDa, close to the theoretical value. These gave strong evidence that both HR121 and HR212 could still assemble into six-helix bundle structures in PBS similar to that formed by 2-helix. However, the six-helix bundles formed by HR121 or HR212 also had three superfluous HR1s or HR2s, which were different from that formed by 2-helix.

Both HR121 and HR212 exhibited helical structure

The biophysical properties of the individual proteins concerned were tested by CD spectrometry as described under Materials and methods. HR121 and HR212 had a CD spectrum exhibiting double minima at 208 and 222 nm while N44-30a and C38-30a were unordered. These indicated that HR121 and HR212 showed a salient α-helix character (Figs. 4A and B). Namely, the two proteins were more stable than single HR1 or HR2.

HR121 could bind to C38-30a in vitro and HR212 could pull down N108-30a

GST-HR121 bound to C38-30a, while it did not bind to N108-30a. GST-HR212 bound to N108-30a, while it did not pull down C38-30a (Figs. 4C and D). Moreover,

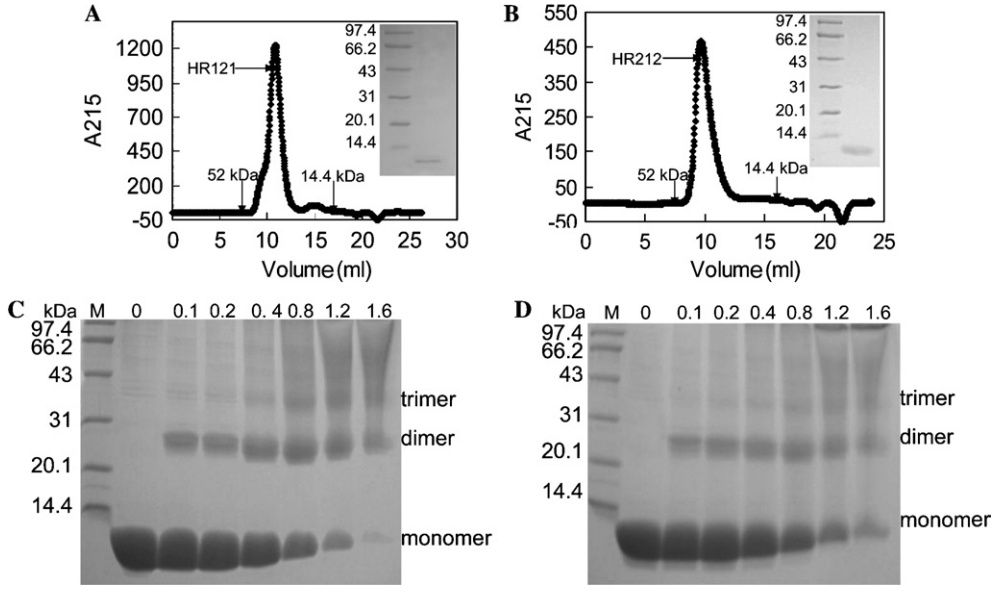

Fig. 3. Gel filtration analysis and chemical cross-linking of the designed proteins. The protein samples were loaded on Superdex G75 column. The relative positions of the standard protein markers are indicated (kDa). (A,B) The gel filtration profiles of HR121 and HR212, respectively. The inset pictures are SDS–PAGE analysis of the sample from the peaks; left: protein markers (kDa); right: the proteins from the peaks. (C,D) Chemical cross-linking of HR121 and HR212, respectively. Protein markers are shown in lane M. The numbers 0, 0.1, 0.2, 0.4, 0.8, 1.2, and 1.6 indicate the concentrations of ethylene glycol bis(succinimidyl succinate) (EGS) in millimolar used. Bands corresponding to monomer, dimer, and trimer are also indicated.

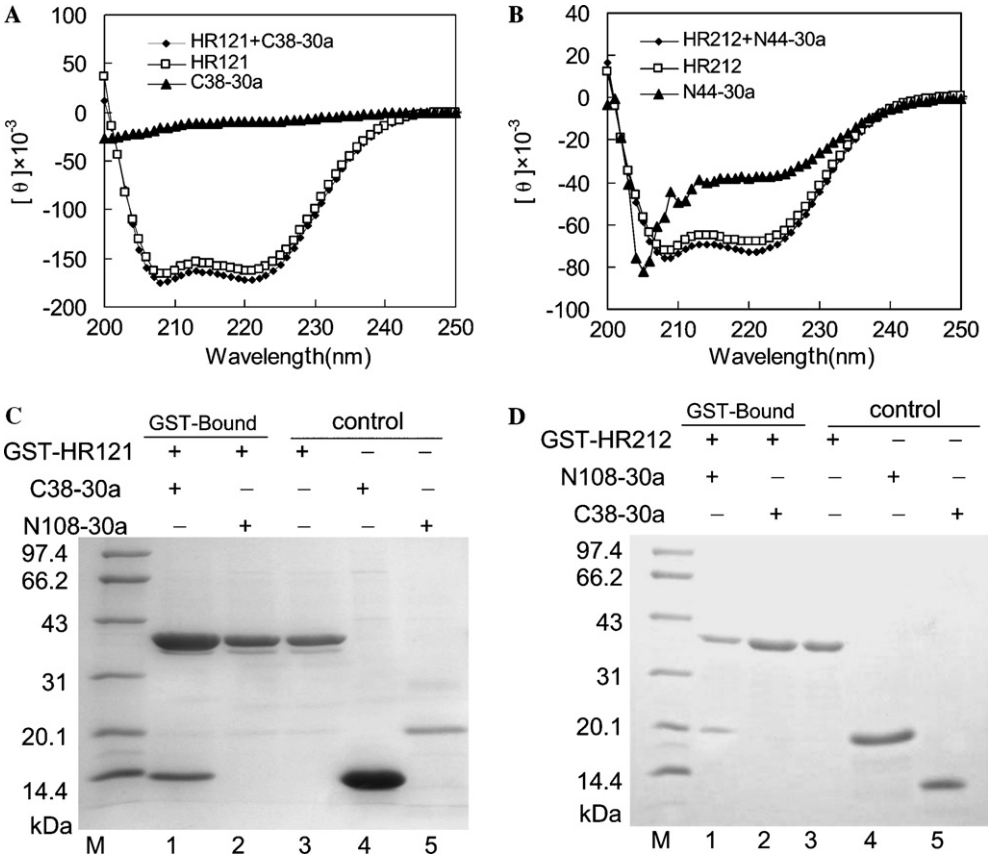

Fig. 4. Analysis of the binding activities of HR121 and HR212 in vitro. (A,B) CD spectra of HR121 and HR212 before and after adding C38-30a and N44-30a. The ellipticities at 208 and 222 nm increased upon mixing HR121 and C38-30a (A), and mixing HR212 and N44-30a also increased the ellipticities at 208 and 222 nm (B). (C) The C38-30a was pulled down by GST-HR121. The results show that GST-HR121 could interact with C38-30a (lane 1), while GST-HR121 could not pull down N108-30a (lane 2); lane 3, purified GST-HR121; lane 4, purified C38-30a; lane 5, purified N108-30a; and lane M, protein markers (kDa). (D) GST-HR212 could interact with N108-30a (lane 1), while GST-HR212 could not pull down C38-30a (lane 2); lane 3, purified GST-HR212; lane 4, purified N108-30a; lane 5, purified C38-30a; and lane M, protein markers (kDa).

GST-HR212 could pull down N44-30a (data not shown). These implied that GST as well as the fusion partner of 50 extra amino acids of N108-30a and C38-30a did not affect the binding activity of HR121 and HR212. The ellipticities at 208 and 222 nm increased upon mixing HR121 with C38-30a and they also increased upon mixing HR212 with N44-30a (Figs. 4A and B). The increase in ellipticity at 208 and 222 nm upon mixing indicated an interaction between the two proteins and the interaction induced a helical conformation. These results showed that HR121 was analogous to its monomer (HR1) that could bind to C38 and HR212 was analogous to HR2.

In this study, N108-30a had a strong tendency to aggregate. It was partially soluble and liable to precipitate in PBS but was soluble in clarified bacterium supernatants while N44-30a was soluble in both PBS and supernatant, but aggregated at high concentration. On the other hand, peptide N44 bound to HR2 region of the spike protein according to the crystal structure [17] and GST-HR212 could pull down N44-30a (data not shown). Due to these two reasons, we analyzed the spectra of N44-30a and the mixture of N44-30a and HR212, not the mixture of N108-30a and HR212 in CD spectra analysis.

However, both HR121 and HR212 were soluble in PBS and they did not aggregate even at high concentration. That is to say, HR121 and HR212 were more stable than their respective analogs, HR1 and HR2.

Both HR121 and HR212 could inhibit HIV/SARS pseudovirus mediated cell fusion

SARS-CoV has been forbidden to be used as experimental materials by the government, so HIV/SARS pseudovirus was used in the cell fusion assays. It is the safe, conformational mimetics of the SARS-CoV [19,31–33]. Both HR121 and HR212 exhibited anti-viral activity (Fig. 5) with IC_{50} values 4.13 ± 0.43 and 0.95 ± 0.12 μM, respectively.

The GST-HR2-38 and HR1-30a constructed in previous study [20] were also tested for the inhibitory activity of HIV/SARS pseudovirus. The IC_{50} value of GST-HR2-38 was 1.02 μM approximate to that of HR212.

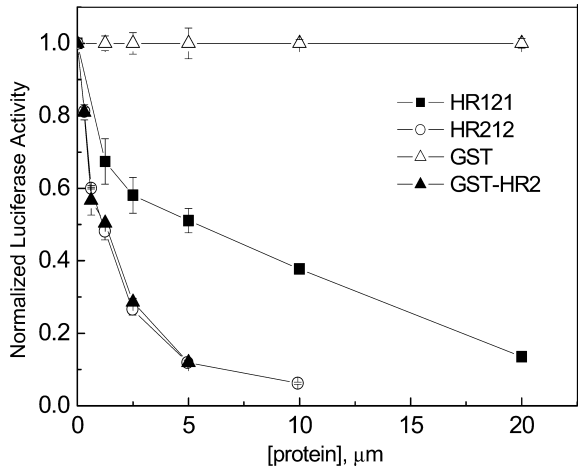

Fig. 5. Titration of viral infectivity by HR121 (filled squares), HR212 (open circles), GST-HR2-38 (filled triangles), and GST (open triangles). The IC_{50} values of HR121, HR212, and GST-HR2-38 in this assay are 4.13 ± 0.43, 0.95 ± 0.12, and 1.02 ± 0.02 μM, respectively. GST protein itself was used as control and no inhibitions were observed. The data represent the means ± SEM of three separate experiments.

However, HR1-30a did not have any effect on virus infection while HR121 (HR1 analog) had fusion inhibitory activity. It was proposed that formation of the bundles (Fig. 1C) was irreversible under physiological conditions. HR121 could reverse at physiological conditions to expose its HR2 segment. The exposed HR2 bound to viral HR1 region and prevented the formation of S2 six-helix bundle, thereby blocking fusion by the same mechanism as that of individual HR2 peptides [21].

Taking all the above into consideration, the designed proteins, HR121 and HR212, inhibited entry of the HIV/SARS pseudovirus and the inhibitory activity of HR212 was comparable to that of HR2. Moreover, the designed proteins were easily purified with the low cost of production and they were more stable than single HR1 or HR2. Accordingly, this design strategy should also be used in other enveloped viruses, especially HIV.

Acknowledgments

We are grateful to Dr. Shibo Jiang of York Blood New Center for critical reading of the manuscript and providing constructive comments and suggestions. This work was supported by grants from National Projects 973 (Grant Nos. G1999075602 and 2001CB510001).

References

[1] K.W. Tsang, P.L. Ho, G.C. Ooi, W.K. Yee, T. Wang, M. Chan-Yeung, W.K. Lam, W.H. Seto, L.Y. Yam, T.M. Cheung, P.C. Wong, B. Lam, M.S. Ip, J. Chan, K.Y. Yuen, K.N. Lai, A cluster of cases of severe acute respiratory syndrome in Hong Kong, N. Engl. J. Med. 348 (2003) 1977–1985.

[2] S.M. Poutanen, D.E. Low, B. Henry, S. Finkelstein, D. Rose, K. Green, R. Tellier, R. Draker, D. Adachi, M. Ayers, A.K. Chan, D.M. Skowronski, I. Salit, A.E. Simor, A.S. Slutsky, P.W. Doyle, M. Krajden, M. Petric, R.C. Brunham, A.J. McGeer, Identification of severe acute respiratory syndrome in Canada, N. Engl. J. Med. 348 (2003) 1995–2005.

[3] H.S. Gao, S.X. Wang, L.M. Chen, Y.M. Li, S.L. Yuan, Z.S. Jiao, W.L. Hui, Z. Yang, Z.Y. Zhao, Analysis of relation between the usage of corticosteroid in treatment and arthralgia as a sequela of SARS patients, Zhongguo Wei Zhong Bing Ji Jiu Yi Xue 16 (2004) 277–280.

[4] M. Eickmann, S. Becker, H.D. Klenk, H.W. Doerr, K. Stadler, S. Censini, S. Guidotti, V. Masignani, M. Scarselli, M. Mora, C. Donati, J.H. Han, H.C. Song, S. Abrignani, A. Covacci, R. Rappuoli, Phylogeny of the SARS coronavirus, Science 302 (2003) 1504–1505.

[5] J.S. Peiris, S.T. Lai, L.L. Poon, Y. Guan, L.Y. Yam, W. Lim, J. Nicholls, W.K. Yee, W.W. Yan, M.T. Cheung, V.C. Cheng, K.H. Chan, D.N. Tsang, R.W. Yung, T.K. Ng, K.Y. Yuen, Coronavirus as a possible cause of severe acute respiratory syndrome, Lancet 361 (2003) 1319–1325.

[6] T.G. Ksiazek, D. Erdman, C.S. Goldsmith, S.R. Zaki, T. Peret, S. Emery, S. Tong, C. Urbani, J.A. Comer, W. Lim, P.E. Rollin, S.F. Dowell, A.E. Ling, C.D. Humphrey, W.J. Shieh, J. Guarner, C.D. Paddock, P. Rota, B. Fields, J. DeRisi, J.Y. Yang, N. Cox, J.M. Hughes, J.W. LeDuc, W.J. Bellini, L.J. Anderson, A novel coronavirus associated with severe acute respiratory syndrome, N. Engl. J. Med. 348 (2003) 1953–1966.

[7] T. Kuiken, R.A. Fouchier, M. Schutten, G.F. Rimmelzwaan, G. van Amerongen, D. van Riel, J.D. Laman, T. de Jong, G. van Doornum, W. Lim, A.E. Ling, P.K. Chan, J.S. Tam, M.C. Zambon, R. Gopal, C. Drosten, S. van der Werf, N. Escriou, J.C. Manuguerra, K. Stohr, J.S. Peiris, A.D. Osterhaus, Newly discovered coronavirus as the primary cause of severe acute respiratory syndrome, Lancet 362 (2003) 263–270.

[8] M.A. Marra, S.J. Jones, C.R. Astell, R.A. Holt, A. Brooks-Wilson, Y.S. Butterfield, J. Khattra, J.K. Asano, S.A. Barber, S.Y. Chan, A. Cloutier, S.M. Coughlin, D. Freeman, N. Girn, O.L. Griffith, S.R. Leach, M. Mayo, H. McDonald, S.B. Montgomery, P.K. Pandoh, A.S. Petrescu, A.G. Robertson, J.E. Schein, A. Siddiqui, D.E. Smailus, J.M. Stott, G.S. Yang, F. Plummer, A. Andonov, H. Artsob, N. Bastien, K. Bernard, T.F. Booth, D. Bowness, M. Czub, M. Drebot, L. Fernando, R. Flick, M. Garbutt, M. Gray, A. Grolla, S. Jones, H. Feldmann, A. Meyers, A. Kabani, Y. Li, S. Normand, U. Stroher, G.A. Tipples, S. Tyler, R. Vogrig, D. Ward, B. Watson, R.C. Brunham, M. Krajden, M. Petric, D.M. Skowronski, C. Upton, R.L. Roper, The genome sequence of the SARS-associated coronavirus, Science 300 (2003) 1399–1404.

[9] P.A. Rota, M.S. Oberste, S.S. Monroe, W.A. Nix, R. Campagnoli, J.P. Icenogle, S. Penaranda, B. Bankamp, K. Maher, M.H. Chen, S. Tong, A. Tamin, L. Lowe, M. Frace, J.L. DeRisi, Q. Chen, D. Wang, D.D. Erdman, T.C. Peret, C. Burns, T.G. Ksiazek, P.E. Rollin, A. Sanchez, S. Liffick, B. Holloway, J. Limor, K. McCaustland, M. Olsen-Rasmussen, R. Fouchier, S. Gunther, A.D. Osterhaus, C. Drosten, M.A. Pallansch, L.J. Anderson, W.J. Bellini, Characterization of a novel coronavirus associated with severe acute respiratory syndrome, Science 300 (2003) 1394–1399.

[10] D.M. Eckert, P.S. Kim, Mechanisms of viral membrane fusion and its inhibition, Annu. Rev. Biochem. 70 (2001) 777–810.

[11] W. Weissenhorn, A. Dessen, L.J. Calder, S.C. Harrison, J.J. Skehel, D.C. Wiley, Structural basis for membrane fusion by enveloped viruses, Mol. Membr. Biol. 16 (1999) 3–9.

[12] J.J. Skehel, D.C. Wiley, Receptor binding and membrane fusion in virus entry: the influenza hemagglutinin, Annu. Rev. Biochem. 69 (2000) 531–569.
[13] J. Bentz, Membrane fusion mediated by coiled coils: a hypothesis, Biophys. J. 78 (2000) 886–900.
[14] B.J. Bosch, R. van der Zee, C.A. de Haan, P.J. Rottier, The coronavirus spike protein is a class I virus fusion protein: structural and functional characterization of the fusion core complex, J. Virol. 77 (2003) 8801–8811.
[15] Z.Y. Yang, Y. Huang, L. Ganesh, K. Leung, W.P. Kong, O. Schwartz, K. Subbarao, G.J. Nabel, pH-dependent entry of severe acute respiratory syndrome coronavirus is mediated by the spike glycoprotein and enhanced by dendritic cell transfer through DC-SIGN, J. Virol. 78 (2004) 5642–5650.
[16] W.R. Gallaher, J.M. Ball, R.F. Garry, M.C. Griffin, R.C. Montelaro, A general model for the transmembrane proteins of HIV and other retroviruses, AIDS Res. Hum. Retroviruses 5 (1989) 431–440.
[17] Y. Xu, Z. Lou, Y. Liu, H. Pang, P. Tien, G.F. Gao, Z. Rao, Crystal structure of SARS-CoV spike protein fusion core, J. Biol. Chem. 279 (2004) 49414–49419.
[18] B.J. Bosch, B.E. Martina, R. Van Der Zee, J. Lepault, B.J. Haijema, C. Versluis, A.J. Heck, R. De Groot, A.D. Osterhaus, P.J. Rottier, Severe acute respiratory syndrome coronavirus (SARS-CoV) infection inhibition using spike protein heptad repeat-derived peptides, Proc. Natl. Acad. Sci. USA 101 (2004) 8455–8460.
[19] K. Yuan, L. Yi, J. Chen, X. Qu, T. Qing, X. Rao, P. Jiang, J. Hu, Z. Xiong, Y. Nie, X. Shi, W. Wang, C. Ling, X. Yin, K. Fan, L. Lai, M. Ding, H. Deng, Suppression of SARS-CoV entry by peptides corresponding to heptad regions on spike glycoprotein, Biochem. Biophys. Res. Commun. 319 (2004) 746–752.
[20] J. Zhu, G. Xiao, Y. Xu, F. Yuan, C. Zheng, Y. Liu, H. Yan, D.K. Cole, J.I. Bell, Z. Rao, P. Tien, G.F. Gao, Following the rule: formation of the 6-helix bundle of the fusion core from severe acute respiratory syndrome coronavirus spike protein and identification of potent peptide inhibitors, Biochem. Biophys. Res. Commun. 319 (2004) 283–288.
[21] S. Liu, G. Xiao, Y. Chen, Y. He, J. Niu, C.R. Escalante, H. Xiong, J. Farmar, A.K. Debnath, P. Tien, S. Jiang, Interaction between heptad repeat 1 and 2 regions in spike protein of SARS-associated coronavirus: implications for virus fusogenic mechanism and identification of fusion inhibitors, Lancet 363 (2004) 938–947.
[22] J.C. Leao, C. Frezzini, S. Porter, Enfuvirtide: a new class of antiretroviral therapy for HIV infection, Oral Dis. 10 (2004) 327–329.
[23] R.M. Markosyan, X. Ma, M. Lu, F.S. Cohen, G.B. Melikyan, The mechanism of inhibition of HIV-1 env-mediated cell-cell fusion by recombinant cores of gp41 ectodomain, Virology 302 (2002) 174–184.
[24] P.Y. Li, J.Q. Zhu, B.L. Wu, F. Gao, P. Tien, Z. Rao, G.F. Gao, Crystallization and preliminary X-ray diffraction analysis of post-fusion six-helix bundle core structure from Newcastle disease virus F protein, Acta Crystallogr. D 59 (2003) 1296–1298.
[25] Y. Liu, J. Zhu, M.G. Feng, P. Tien, G.F. Gao, Six-helix bundle assembly and analysis of the central core of mumps virus fusion protein, Arch. Biochem. Biophys. 421 (2004) 143–148.
[26] J. Zhu, C.W. Zhang, Y. Qi, P. Tien, G.F. Gao, The fusion protein core of measles virus forms stable coiled-coil trimer, Biochem. Biophys. Res. Commun. 299 (2002) 897–902.
[27] J.Q. Zhu, C.W. Zhang, Z. Rao, P. Tien, G.F. Gao, Biochemical and biophysical analysis of heptad repeat regions from the fusion protein of Menangle virus, a newly emergent paramyxovirus, Arch. Virol. 148 (2003) 1301–1316.
[28] M. Singh, B. Berger, P.S. Kim, LearnCoil-VMF: computational evidence for coiled-coil-like motifs in many viral membrane-fusion proteins, J. Mol. Biol. 290 (1999) 1031–1041.
[29] B. Tripet, M.W. Howard, M. Jobling, R.K. Holmes, K.V. Holmes, R.S. Hodges, Structural characterization of the SARS-coronavirus spike S fusion protein core, J. Biol. Chem. 279 (2004) 20836–20849.
[30] H.K. Deng, D. Unutmaz, V.N. KewalRamani, D.R. Littman, Expression cloning of new receptors used by simian and human immunodeficiency viruses, Nature 388 (1997) 296–300.
[31] P. Wang, J. Chen, A. Zheng, Y. Nie, X. Shi, W. Wang, G. Wang, M. Luo, H. Liu, L. Tan, X. Song, Z. Wang, X. Yin, X. Qu, X. Wang, T. Qing, M. Ding, H. Deng, Expression cloning of functional receptor used by SARS coronavirus, Biochem. Biophys. Res. Commun. 315 (2004) 439–444.
[32] Y. Huang, Z.Y. Yang, W.P. Kong, G.J. Nabel, Generation of synthetic severe acute respiratory syndrome coronavirus pseudoparticles: implications for assembly and vaccine production, J. Virol. 78 (2004) 12557–12565.
[33] H. Zhang, G. Wang, J. Li, Y. Nie, X. Shi, G. Lian, W. Wang, X. Yin, Y. Zhao, X. Qu, M. Ding, H. Deng, Identification of an antigenic determinant on the S2 domain of the severe acute respiratory syndrome coronavirus spike glycoprotein capable of inducing neutralizing antibodies, J. Virol. 78 (2004) 6938–6945.